Origin of carrier localization on two-dimensional GaN substitution layers embedded in GaAs

Heidemarie Schmidt
Faculty of Physics and Geosciences, University of Leipzig, Linnéstraße 3-5, 04103 Leipzig, Germany

Georg Böhm
Institute for Surface Modification (IOM), Permoserstraße 15, 04303 Leipzig, Germany

(Received 28 June 2002; revised manuscript received 24 February 2003; published 17 June 2003)

The electronic properties of GaAs containing a two-dimensional GaN substitution layer are studied by means of the empirical pseudopotential method in a periodic modeling approach. These are found to be anomalous compared with A(III)-B(V) semiconductors containing other two-dimensional substitution layers, i.e., not only *one* but *two* states in the lower conduction-band region of the GaAs host material are perturbed. It is shown that this anomaly originates from chemical and size effects associated with the embedded GaN substitution layer. The theoretical results can be correlated with first experimental investigations on the GaN/GaAs system.

DOI: 10.1103/PhysRevB.67.245315 PACS number(s): 71.15.Dx, 71.55.Eq

I. INTRODUCTION

(001) superlattices with one isovalent atomic substitution layer, for example, GaP/InP, InP/GaP, InAs/GaAs, and GaN/GaAs, are perfectly ordered GaInP, InGaP, InGaAs, and GaNAs alloys, respectively. Only recently, it has been shown by the photoluminescence, absorption, and reflection measurements that the optical properties of a host material can be drastically modified by embedding isovalent atomic substitution layers.[1–4] Optoelectronic devices of A(III)-B(V) semiconductors with quantum layers in the active region are of great importance owing to their efficient optical excitonic transitions. The efficiency of excitonic transitions increases with increasing exciton localization, i.e., with a decreasing quantum layer thickness. Therefore, the extreme case of atomic substitution layers in the active region is expected to play a crucial role for next generation optical devices.

In Refs. 5,6, it was investigated how the modifications of the optical properties of GaP/InP, InP/GaP, InAs/GaAs, and GaN/GaAs depend on the chemical and size effects associated with the embedded atomic substitution layer. Special attention was paid to the localization properties of electron and hole states and to the question whether excitons can be effectively bound to the atomic substitution layer. As already pointed out in Ref. 6, among the systems mentioned above, the GaN/GaAs system which incorporates material components with the greatest difference in size and chemistry is the only one that shows anomalous electronic properties.

There have been many attempts to fabricate damage free GaN/GaAs single heterostructures. These efforts were motivated by the search for a robust GaAs surface passivation material using helicon-wave-excited N_2-Ar plasma treatments,[7] by the possibility to produce GaN/GaAs diodes by plasma-assisted molecular-beam epitaxy[8] or by GaN wafer fusion.[9] Cubic GaN has some advantages compared with hexagonal GaN, namely, easy cleavage and higher carrier mobility. However, due to the inferior crystal quality and the obstructing mixing of hexagonal GaN, reports on the optical and electrical properties of single GaN/GaAs heterostructures vary considerably in dependence on growth condition. For example, in Ref. 10, it was found that the GaN/GaAs heterojunction behaves either as a back-to-back diode structure or as a metal-insulator-semiconductor structure depending on the GaAs substrate growth temperature. This shows that in order to realize the integration of GaN and GaAs optoelectronic devices or to evaluate the potential applications for GaN as an insulating or passivating material for GaAs, a theoretical investigation of the electrical and optical properties of the GaN/GaAs system is of great importance.

In the present work, we study the electronic band structure of the GaN/GaAs double heterojunction and compare it with the corresponding band structure of the unordered GaAsN alloy. It should be noted that, in contrast to unordered GaAsN alloys,[11,12] in GaN/GaAs systems, efficient optical transitions have not been achieved yet. Unordered GaAsN is well known as an ''anomalous'' alloy because its two lowest conduction-bands E_0 and E_+ possess large, composition-dependent bowing coefficients and show an abrupt increase in the effective mass. For example, this has been observed experimentally in GaAsN/GaAs quantum wells[13,14] and has been explained in terms of a band anticrossing model.[15] However, the band anticrossing model conflicts with detailed band structure calculations,[16–18] which clearly demonstrate that the $a_1(L_{1c})$ resonance and not the $a_1(N)$ resonance, which is induced by isolated N impurities, is the principal source of the additional strong E_+ transition. The observation of anomalies in both GaN/GaAs and GaAsN alloys leads us to the conclusion that (001) ordering of ''anomalous'' alloys does not remove their band-structure anomalies.

First theoretical investigations on GaN/GaAs were performed by Hjalmarson (Ref. 19), focusing on the short-range potential produced by the GaN substitution layer and disregarding completely the substitution layer relaxation. As a result, Hjalmarson has found a single electron eigenstate, ca. 300 meV, below the GaAs fundamental band gap that is localized on the GaN substitution layer. By means of the empirical pseudopotential (EPP) method in a periodic modeling approach, we demonstrate that in order to correctly describe the perturbation of the GaAs host material band structure, the

huge GaN/GaAs lattice mismatch has to be included into the calculation. The smallest *N* content in our model supercells amounts to 6.6 %. We find a single electron eigenstate, ca. 850 meV, below the GaAs band gap. This conduction-band minimum (CBM) is localized on the GaN substitution layer and shows strong mixing effects with *X* and *L* states of the host material. Furthermore, we find that the second lowest conduction band (CB1) is also localized on the GaN layer. While the energetical position of CBM is independent of the GaN relaxation, that of CB1 increases with increasing relaxation. The electronic properties of CBM and CB1 of GaN/GaAs can be correlated with those of the lowest conduction-band state E_0 and the N impurity state $a_1(N)$ of GaAsN, respectively.

Our theoretical results can also be correlated with the results of first experimental investigations. By means of temperature-dependent $I(U)$ measurements on single barrier *n*- and *p*-type GaAs/(2.5 nm GaN)/GaAs heterostructures, Huang *et al.* (Ref. 20) have shown that the $I(U)$ characteristics of the *n*-type samples exhibit ''anomalous'' behavior, which may indicate an impurity or a defect-assisted tunneling process through a deep electron level in the GaN quantum layer. Sato (Ref. 21) has measured intense low-temperature photoluminescence from an atomic nitrogen layer embedded in GaAs at 1.43 eV, i.e., 90 meV below the GaAs band-gap energy. We suggest that this photoluminescence originates from an optical transition between the localized CB1 and the GaAs valence-band maximum.

The work is organized as follows. After a brief representation of the theoretical settings in Sec. II, we discuss the band structure of the GaN/GaAs system in Sec. III A, and investigate the physical origin of the observed anomalies in Sec. III B. We conclude with a summary.

II. THEORETICAL SETTINGS

The EPP calculations can be used for demanding band-structure calculations, as, for example, for semiconductor random alloys, superlattices, or quantum dots, provided that the pseudopotential parameters are transferable and continuous in the reciprocal space.[22] It was only recently that such pseudopotentials have been applied for band structure calculations of short-period superlattices.[5,6,22,23] For the ionic potentials, we use a continuous description based on a simple empty core model.[24] The crystal potential is obtained by screening the ionic potential using the static limit of the model dielectric function derived for semiconductors by Levine and Louie.[25] As in Refs. 5,6, in order to achieve the closest agreement between the calculated band structure and low-temperature transition energies and deformation potentials, the EPP parameters of zincblende type GaN and GaAs are determined by a fitting procedure. Spin-orbit (SO) coupling effects at the Γ point are included by means of the quasicubic model.[26] Table I contains the measured lattice constant and the static dielectric constant, which enter the EPP calculation. As can be seen in this table, the experimental low-temperature transition energies are reproduced up to more than 5 eV above the valence-band maximum (VBM). To the best of our knowledge, for GaN zincblende material (β-GaN), apart from the band-gap energy $E(\Gamma_1^c) = 3.37$ eV,[32] experimentally determined fundamental transition energies do not exist. Our calculated $E(X_1^c)$ and $E(L_1^c)$ transition energies amount to 4.48 eV and 5.26 eV (Table I), respectively, and are close to those calculated by Fan *et al.* (Ref. 33). The calculated deformation potentials coincide with the experimental ones and reproduce the great stiffness of GaN.

TABLE I. Calculated and experimental (in brackets) values of the fundamental low-temperature transition energies in units of eV, of the lattice constant *a* in units of Å, the static dielectric constant ϵ_0, of the SO-coupling parameter Δ_{SO} in units of eV, and of the deformation potentials in units of 10^{-6} eV bar^{-1}. All transition energies refer to the top of the (SO-coupling corrected) VBM. In our calculations, the SO coupling which lifts the degeneracy of the sixfold degenerate Γ_{15}^v state has been included by means of the quasicubic model.

	GaN	GaAs
Γ_1^c	3.38 (3.37)	1.52 (1.52)
Γ_{15}^c	10.21	4.63 (4.72)
X_5^v	−2.48	−2.13 (−2.83)
X_1^c	4.48	1.99 (1.98)
X_3^c	6.14	2.35 (2.35)
L_3^v	−0.85	−0.92 (−1.27)
L_1^c	5.26	1.80 (1.81)
a	(4.500)	(5.653)
ϵ_0	(9.50)	(12.4)
Δ_{SO}	(0.015)	(0.340)
$\frac{d}{dp}\Gamma_1^c$	4.0 (4.0)	10.0 (10.7)
$\frac{d}{dp}X_1^c$	0.1	−1.0 (−1.3)
$\frac{d}{dp}L_1^c$	3.8	3.0 (2.8)

[a]Reference 32.
[b]Reference 27.
[c]From wurtzite GaN (Ref. 28).
[d]Reference 29.
[e]Reference 30. All the other experimental data are taken from Ref. 31.

Our continuous EPP parameters are chosen to fulfill the Hartree relation for the mean valence electron potential at $q=0$ (Ref. 34)

$$V_0 = -\lim_{q\to 0}\frac{8\pi(z_a+z_c)}{\Omega_0 q^2}\left(\frac{1}{\epsilon(q)}-\frac{1}{\epsilon_0}\right), \tag{1}$$

where Ω_0, z_a, and z_c denote the unit cell volume, the effective anionic charge, and effective cationic charge, respectively. On the basis of local empirical pseudopotentials, we have calculated the energy of the top of the valence band with respect to the mean potential *V* and have obtained the ionization energy

$$I = -VBM - V - \frac{\Delta_{SO}}{3} \tag{2}$$

which permits to fit the all-important valence-band offsets between different materials. Here, VBM has been corrected by Δ_{SO}, and V has been calculated by means of a relation that includes the Hartree potential [Eq. (1)] corrected by exchange and correlation.[35] The ionization energy for unstrained GaAs and GaN amounts to 5.22 eV and 7.65 eV, respectively, and is in good agreement with the corresponding experimentally determined ionization energies of 5.50 eV (Ref. 36) and 6.67 eV.[37] For unstrained GaN layers embedded in GaAs, the calculated ionization energies propose a type II valence-band and a type I conduction-band alignment. A type II valence-band alignment has also been predicted by Wei and Zunger using first-principles all-electron methods.[38]

The parameter to deal with at the boundaries of the heterojunction in *microscopic* calculations is the EPP screening function. In our case, the ionic potentials of Ga in the substitution layer and host material are identical. This allowed us to derive a condition which determines uniquely the EPP screening function at the boundary.[6] Furthermore, in order to study the influence of layer thickness and electronic coupling, we have used (001)-supercell structures. These supercells mimic a periodic arrangement of GaN substitution layers in the GaAs host material, where the in-plane atomic positions are fixed by the GaAs lattice. For detailed investigations of the influence of strain (size effect) and crystal field potential (chemical effect) on the energy band structure of the host material, we have considered three differently composed supercell structures. Let us indicate the number of strained or unstrained monolayers (ML's) of a supercell by the index n,s or n,us, respectively. For example, $GaN_{1,s}/GaAs_{14,us}$ denotes a 15 ML (001)-supercell structure containing 1 tensile strained GaN ML and 14 unstrained GaAs MLs. In order to investigate the influence of chemical effects and of size effects separately, we have calculated the energy band structure of $GaN_{1,us}/GaAs_{14,us}$ and $GaAs_{1,s}/GaAs_{14,us}$, respectively. We have also examined how the energy band structure of the GaAs host material is influenced by Brillouin-zone (BZ) folding effects using the—actually not realistic—supercell $GaAs_{15,us}$. We describe the strain in the atomic substitution layer by a step model, i.e., we assume that only the vertical spacing $d_\perp$ between the nearest arsenic atomic layers above and below the nitrogen atomic layer is changed due to the interface normal stress. In the step model, the lattice constant of the nitrogen atomic layer along the (001) direction, $a_\perp = 2 \times d_\perp$, can be estimated from the elastic constants c_{11} and c_{12} of GaN using the continuum elasticity theory:[39]

$$a_\perp = 0.5 a_\delta (1 + \epsilon_\perp) = 0.5 a_\delta \left(1 - \frac{2c_{12}}{c_{11}} \epsilon_\parallel \right). \tag{3}$$

We find $d_\perp^E = 0.575a/2$ (Table II). However, our calculations show that for any value $d_\perp^{PP} \leqslant 0.615a/2$, the band gap is closed. Since this has not been observed experimentally,[21] we are led to the conclusion that the continuum elasticity theory does not hold for the GaN/GaAs system. This is not unexpected, because of the large lattice mismatch the critical thickness for the relaxation of strained GaN layers by the creation of dislocation is less than 1 ML.[41] Therefore, the intended damage free GaN/ GaAs single heterostructures can only partially be realized,[8,41–43] whereby the tensile strain of the partially grown GaN layers varies in dependence on the growth conditions. In this work, we study the chemical and size effects in an ideal two-dimensional GaN layer embedded in GaAs for a wide range of strain, i.e., in the whole $d_\perp$ range, $1.00a/2 \geqslant d_\perp \geqslant 0.615a/2$, and find a similar band-structure anomaly. Thus, without loss of generality, we can study the origin of these anomalies by investigating the charge-carrier localization and the spectral projection of band-gap states for a fixed $d_\perp$ value. We chose $d_\perp = 0.900$ $a/2$ because then the calculated band gap of the $GaN_{1,s}/GaAs_{14,us}$ supercell meets the results of photoluminescence investigations on a single GaN ML embedded in GaAs.[21]

TABLE II. Elastic constants c_{11}, c_{12} of the GaN substitution layer material in 10^{11} dyn cm^{-2}, the vertical spacing parameter $d_\perp^E$ derived from continuum elasticity theory in units of $a/2$, and the $d_\perp^{PP}$ value used in the EPP calculations in units of $a/2$ with $a = 5.653$ Å. The grown-in biaxial strain $\epsilon_\parallel$ (%) in the substitution layer of the GaN/GaAs system is expected to be sufficient to cause substantial departure from harmonicity.

System	$\epsilon_\parallel$	c_{11}	c_{12}	$d_\perp^E$	$d_\perp^{PP}$
GaN/GaAs	+25.6	29.300[a]	15.900 [a]	0.575	0.900

[a]Reference 40.

The probability function $\rho_{n,\mathbf{k}}(\mathbf{r})$ for electrons in band n and state $\mathbf{k}$ has been determined by means of the *folded spectrum method*[44] that allows the diagonalization of huge matrices. For $GaAs_{15,us}$ supercells containing identical ML's, the probability density of those supercell eigenstates that belong to the subset of zincblende eigenstates is the same in every GaAs ML of the supercell. On the other hand, in supercell structures containing the nitrogen atomic substitution layer, the energy bands are broken and separated from each other by minigaps at the edges of the minizone and folded eigenstates are formed. Therefore, these superlattices behave like bulk media with anisotropic transport and optical properties. In general, the probability functions of supercell eigenstates possess only the lower symmetry of the supercell, i.e., these are mirrored at the substitution layer. If the charge density probability function $\rho_{n,\Gamma}(\mathbf{r}) = e|\psi_{n,\Gamma}|^2$ of a folded supercell eigenstate $\psi_{n,\Gamma}$ would reveal a localization or a depletion around the substitution layer, $\psi_{n,\Gamma}$ could be regarded as an excited state of the substitution layer or host material, respectively. To decide this, we have investigated the probability function of all band-edge supercell eigenstates.

In order to enhance the features due to the substitution layer, it is common[45] to integrate the square of the wave function in the planes perpendicular to z, thus obtaining $\overline{\rho}(z)$ which still shows strong atomic bulklike oscillations. By averaging $\overline{\rho}(z)$, one obtains the macroscopic averaged charge

TABLE III. Calculated normalized integral $\overline{\overline{\rho}}_{int}$ from which the redistribution of charge carriers in the VBM, CBM, and CB1 around the GaN substitution layer in the GaN/GaAs system can be derived. Charge carriers are localized or delocalized around the substitution layer for $\overline{\overline{\rho}}_{int} > 0.1\overline{3}$ or for $\overline{\overline{\rho}}_{int} < 0.1\overline{3}$, respectively.

GaN/GaAs	$GaAs_{1,s}/GaAs_{14,us}$	$GaN_{1,s}/GaAs_{14,us}$	$GaN_{1,us}/GaAs_{14,us}$
CB1	0.407	0.747	0.665
CBM	0.754	0.555	0.470
VBM	0.104	0.008	0.011

density $\overline{\overline{\rho}}(z)$ (Ref. 45) that clearly shows the effects of the substitution layer. In addition, we have integrated $\overline{\overline{\rho}}(z)$ around the substitution layer within one-lattice constant and have divided it by a normalization factor of 120 (number of electrons per unit cell). This normalized integral will be referred to as $\overline{\overline{\rho}}_{int}$ (Table III). Since the supercells have 15 ML, a $\overline{\overline{\rho}}_{int}$ value above or below $\frac{2}{15}=0.1\overline{3}$ indicates the carrier localization or carrier depletion, respectively, around the substitution layer.

In order to analyze the character of the GaN/GaAs supercell states, we use the spectral projection

$$P_i(\mathbf{k}) = \sum_n |\langle \psi_i(\mathbf{r}) | \phi_{n,\mathbf{k}}(\mathbf{r}) \rangle|^2$$

$$= \sum_n \sum_{\mathbf{G}} |\langle \psi_i(\mathbf{r}) | a_{n,\mathbf{k}}(\mathbf{G}) u_{\mathbf{G},\mathbf{k}}(\mathbf{r}) \rangle|^2 \qquad (4)$$

of the supercell eigenfunctions $\psi_i(\mathbf{r})$ to the zincblende eigenfunctions $\phi_{n,\mathbf{k}}(\mathbf{r})$. Since our supercell wave functions generally do not show the translational invariance of zincblende host crystal states, we calculate the spectral projection using Eq. (4) only at those discrete reciprocal lattice points $\mathbf{k}$, which are folded to the Γ point. By distinguishing between the Γ point and reciprocal lattice points $\mathbf{k}$ along the L and X direction, we also calculate the $\Gamma/X/L$ decomposition. Note that Eq. (4) is analogous to the spectral projection used for GaAsN alloys[46,47,17] with the only difference that in the case of alloys, $\mathbf{k}$ might be any wave vector inside the first Brillouin zone. If there is a single dominant $\mathbf{k}$ point, which contains the majority of the spectral weight of $P_i(\mathbf{k})$, then in the real space the supercell eigenstate $\psi_i(\mathbf{r})$ looks like a linear combination of crystal Bloch states $\phi_{n,\mathbf{k}}$ for the dominant $\mathbf{k}$. As an illustration, in Fig. 1, we show the discrete reciprocal lattice points used for the calculation of the spectral projection of the wave functions for a 3 ML (001) supercell.

III. RESULTS

A. GaN/GaAs-band-structure anomalies

The eigenvalues $E_{n,\Gamma}$ of various 15 ML (001) supercells have been calculated in dependence on size and chemical effects. The corresponding energy bandstructure of four different 15 ML (001) supercells is shown in Fig. 2. The fourfold degenerate VBM and the twofold degenerate CBM of GaAs zincblende material can be seen in the energy band structure of the $GaAs_{15,us}$ supercell (''host'' in Fig. 2). The energetical positions of the former GaAs zincblende eigenstates, i.e., the heavy-hole (hh), light-hole (lh), and spin-orbit split-off (so) state, and of CBM and CB1 are summarized in Table IV. Here, the SO-coupling correction by means of the quasicubic model[26] is included.

The band-gap energy of the $GaAs_{1,s}/GaAs_{14,us}$ structure (''size'' in Fig. 2) is slightly enlarged to 1.641 eV due to the single strained GaAs ML. The bandgap energy of the $GaN_{1,us}/GaAs_{14,us}$ structure (''chemistry'' in Fig. 2) is reduced to 0.660 eV. The corresponding band-gap reduction of 859 meV is much larger than the 300 meV calculated by Hjalmarson.[19] As already expected from the natural type II and type I band offsets in the GaN/GaAs system,[38] we notice that the substitution of a single atomic As layer by an atomic N layer has particular influence on the conduction-band region of the GaAs host material. In the $GaN_{1,s}/GaAs_{14,us}$ supercell (''size & chemistry'' in Fig. 2), both structural and chemical effects are taken into account. For this system, we have calculated a band-gap energy of 0.775 eV, i.e., a band-gap reduction (BGR) of 744 meV. Note that this BGR is 115 meV smaller than that of the $GaN_{1,us}/GaAs_{14,us}$ structure. Actually, one should expect that the atomic N layer influences the energy band structure of the GaAs host material in still lower conduction-band regions, because for GaN lattice matched to GaAs, the biaxial strain-modified natural type II and type I band offsets increase to 0.875 eV and 1.852 eV[48], respectively.

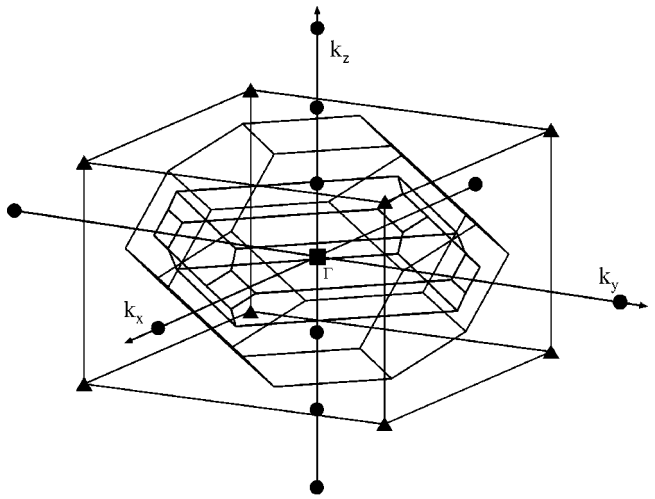

FIG. 1. First Brillouin zone of a zincblende lattice and of a 3 ML (001) supercell. The reciprocal lattice points $\mathbf{k}$ along the L-(▲) and X-(●) directions, which are used for the spectral projection of the 3 ML (001) supercell wave functions, are indicated.

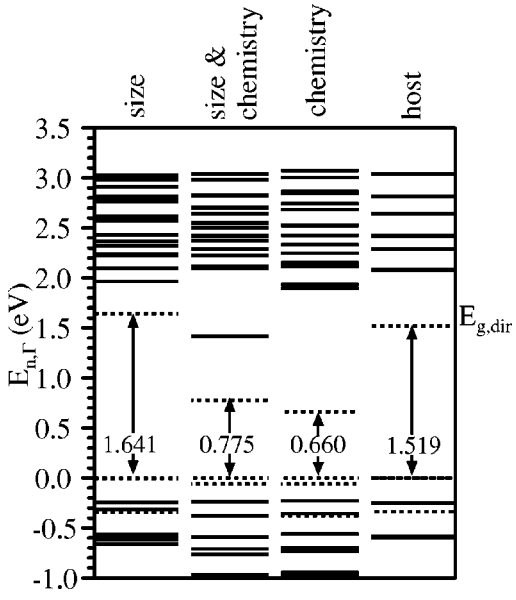

FIG. 2. Γ-point eigenstates in the energy region from −1.0 to 3.5 eV (with SO-coupling correction) of four different 15 ML (001) supercells of the GaN/GaAs system. The VBM is set to zero on energy scale. We distinguish between folded supercell states (continuous lines) and former zincblende states (dotted lines). The energetical position of the former zincblende states can be well recognized from the supercell structure in the right panel (host) which is used to investigate the influence of BZ folding. The realistic supercell structure (size & symmetry) has a huge band-gap reduction (BGR) of 744 meV. Note that the second lowest conduction-band (continuous line) will be identified as an excited state of the GaN substitution layer later on. The hypothetical supercell structures (size resp. chemistry) are used to investigate the influence of strain (size) and exchange of atomic potentials (chemistry).

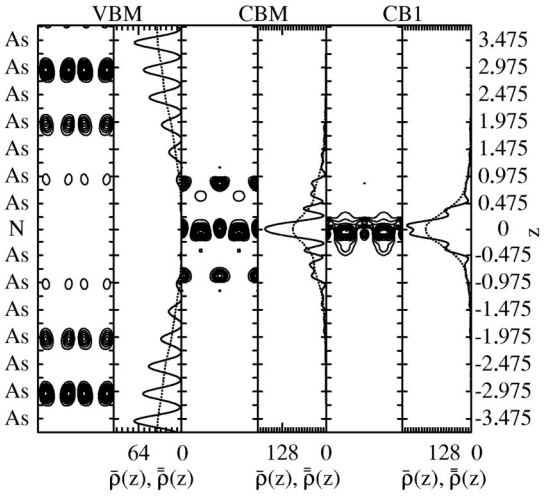

FIG. 3. Γ-point probability function of charge-density of the GaN/GaAs structure in units of *e* per unit cell. Left panel: highest valence band (VBM); middle panel: lowest conduction-band (CBM); and right panel: second lowest conduction-band (CB1). Each panel's left column depicts the contour plot of $\rho(\mathbf{r})$ of two unit cells in the (110) plane. The *z* axis along [001] and the [110] axis cover a segment of $7.5\,a$ and $\sqrt{2}\,a$, respectively. [The contour step for $\rho(\mathbf{r})$ of the VBM, CBM, and CB1 amounts to 0.032, 0.040, and 0.065, respectively.] The right columns present the integral electronic charge-density $\overline{\rho}(z)$ (solid line), spatially averaged over the *x* and *y* directions, i.e., over the (110) plane, and the macroscopic averaged charge-density $\overline{\overline{\rho}}(z)$ (scattered line).

In order to study the localization properties of the VBM, CBM, and CB1 band-edge eigenstates, we have determined the charge-density probability function $\rho_{n,\Gamma}(\mathbf{r}) = e|\psi_{n,\Gamma}|^2$ up to 5 eV above the VBM of the GaN/GaAs system (Fig. 3) in dependence on size (Fig. 4) and chemistry (Fig. 5). The charge-density probability function of a given 15 ML (001)-supercell eigenstate is normalized to (15×8=120) electrons/unit cell. The contour plots of the charge-density distribution in the $\overline{\Gamma}_3^v$ (VBM) and $\overline{\Gamma}_1^c$ (CBM) state are represented in the (110)-plane of the superlattice in Figs. 3, 4, and 5. The represented section of the (110) plane cuts a whole and two half primitive unit cells that lie diagonally in this plane. The calculated $\rho_{n,\Gamma}$ of the VBM, CBM, and CB1 (Fig. 3) reveal that the charge carriers in VBM are depleted around the GaN substitution layer. On the other hand, the center of the charge-density (CCD) of the CBM and CB1 of $GaN_{1,s}/GaAs_{14,us}$ amounts to $0.56\,a$ and $0.37\,a$, respectively. This means that electrons in CBM and CB1 of the GaN/GaAs system are strongly localized around the GaN substitution layer, the CCD being even slightly smaller than one-lattice constant *a*. The normalized integrals $\overline{\overline{\rho}}_{int}$ are given in Table III. Observe the similarities in the contour

TABLE IV. Calculated energetical position of the two localized conduction-band states CBM and the CB1 and of the former hh, lh, and so zincblende eigenstates of the host material at the Γ point in units of eV. The three highest valence bands are denoted by E_1, E_2, and E_3. The energetical position of the CBM corresponds to the value of $E_{g,dir}$ because the energetical position of E_1 is set to zero on energy scale. Note that for $GaAs_{1,s}/GaAs_{14,us}$ (one biaxial tensile strained GaAs ML), the states E_1 and E_2 correspond to the former lh and hh eigenstates, respectively, whereas for all the other supercells the states E_1 and E_2 correspond to the former hh and lh eigenstates, respectively.

	$GaAs_{1,s}/GaAs_{14,us}$	$GaN_{1,s}/GaAs_{14,us}$	$GaN_{1,us}/GaAs_{14,us}$	$GaAs_{15,us}$
$E_{g,CB1}$	1.965	1.416	1.897	2.081
$E_{g,dir}$	1.641	0.775	0.660	1.519
E_2	−0.006	−0.059	−0.059	0.000
E_3	−0.343	−0.380	−0.380	−0.340

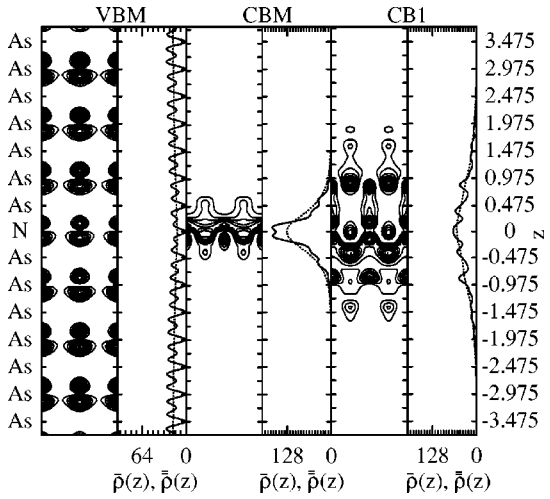

FIG. 4. Γ-point probability function of the 15 ML (001)-supercell in dependence on the size effect with a contour step of 0.015, 0.053, and 0.020 for $\rho(\mathbf{r})$ of the VBM, CBM, and CB1, respectively. The *z* axis has the same scaling as that in Fig. 3. See the explanations in Fig. 3.

plots of the charge densities, for example, of CB1 in Fig. 3, CBM in Fig. 4, and CB1 in Fig. 5. This indicates that the corresponding wave functions have a similar character. For the $GaN_{1,s}/GaAs_{14,us}$ structure, where structural and chemical effects are superimposed, one would expect that the localization of charge carriers in the CBM is stronger than that of the $GaN_{1,us}/GaAs_{14,us}$ (only chemical effects) and $GaAs_{1,s}/GaAs_{14,us}$ (only size effects) structures. However, this superposition rule does not hold. Probably, this is due to a strong mixing of band-edge conduction-band states. Indeed, we have found such a strong mixing by applying the spectral projection method in Sec. III B.

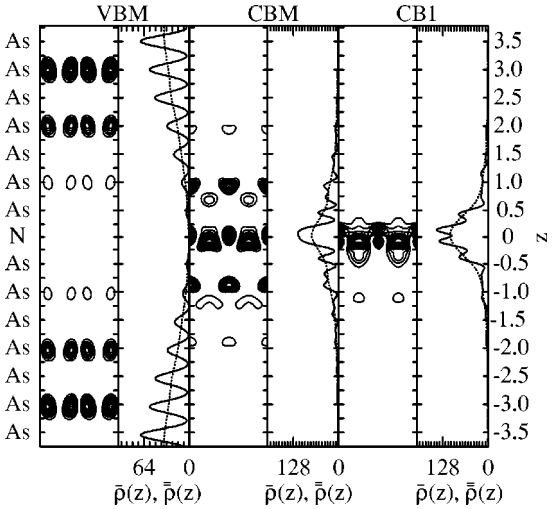

FIG. 5. Γ-point probability function of the 15 ML (001) supercell in dependence on the chemical effect with a contour step of 0.029, 0.030, and 0.049 for $\rho(\mathbf{r})$ of the VBM, CBM, and CB1, respectively. Observe that the scaling of the *z* axis differs from that of Figs. 3 and 4 because the supercell is not strained here. See the explanations in Fig. 3.

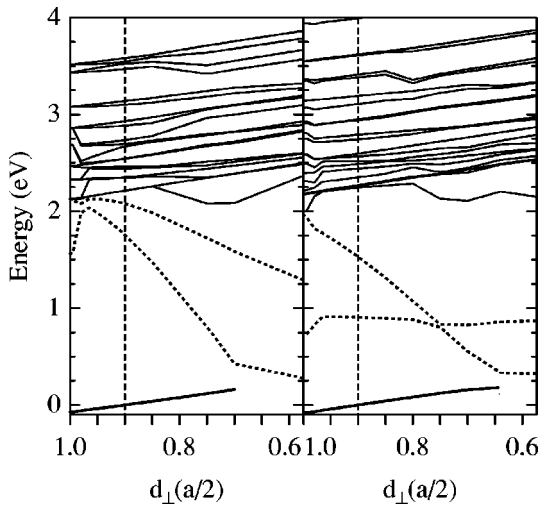

FIG. 6. Γ-point eigenstates of the $GaAs_{1,s}/GaAs_{14,us}$ structure (left panel) and the $GaN_{1,s}/GaAs_{14,us}$ structure (right panel) in eV in dependence on the vertical spacing parameter $d_\perp$ (without so-coupling correction). $d_\perp$ varies from $a/2$, i.e., unstrained substitution layer, to 0.6 $a/2$. Because the VBM is set to zero on energy scale for the $d_\perp$ value of 0.9 $a/2$, the influence of size effect on CBM and CB1 (dotted lines) can be well compared with Fig. 2.

B. Origin of band-structure anomaly

In order to investigate the physical origin of the band-structure anomaly of the GaN/GaAs system, we have analyzed how this anomaly depends on size (Fig. 6) and chemical (Fig. 7) effects. The influence of the size effect has been modeled by varying the vertical spacing parameter of the nitrogen substitution layer in $GaN_{1,s}/GaAs_{14,us}$ from $d_\perp = a/2$ (unstrained substitution layer) to $d_\perp = 0.6\ a/2$ (Fig. 6, right panel). Because the calculated band gap closes at $d_\perp = 0.76\ a/2$, the energetical position of the VBM can only be calculated for $d_\perp > 0.76\ a/2$.

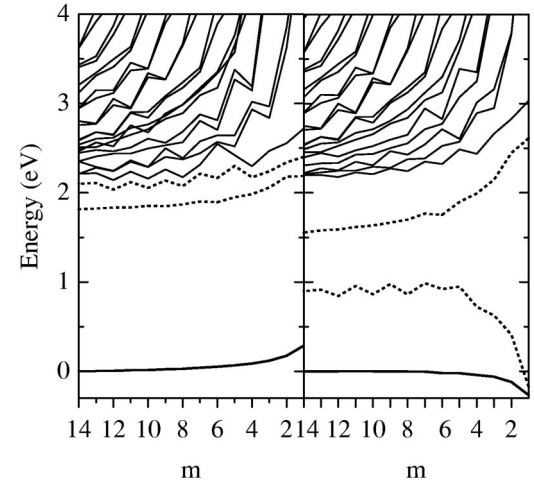

FIG. 7. Γ-point eigenstates of the $GaAs_{1,s}/GaAs_{m,us}$ structure (left panel) and the $GaN_{1,s}/GaAs_{m,us}$ structure (right panel) given in eV in dependence on the number *m* of unstrained host material ML (without SO-coupling correction). *m* varies from 2 to 14. Because the VBM is set to zero on energy scale for $m = 14$, the influence of the chemical effect on the CBM and CB1 (dotted lines) can be well compared with Fig. 2.

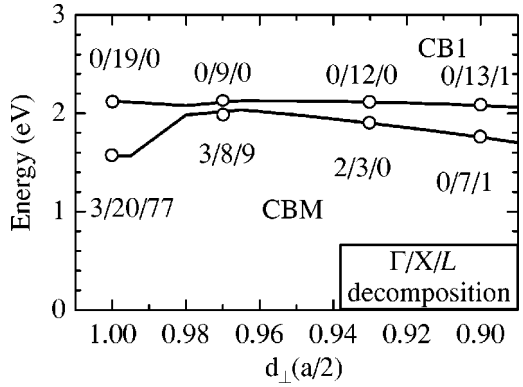

FIG. 8. Energetical position of the CBM and CB1 of $GaAs_{1,s}/GaAs_{m,us}$ (Fig. 6, left panel) in dependence on the vertical spacing parameter $d_\perp$ (without so-coupling correction) where $d_\perp$ varies from $a/2$ to 0.9 $a/2$. The corresponding $\Gamma/X/L$ spectral decomposition is given for $d_\perp = 1.00, 0.97, 0.93$, and 0.90 $a/2$. Here, the latter two decomposition values measure the X and L couplings due to Brillouin-zone folding and size effects (not to chemical effects).

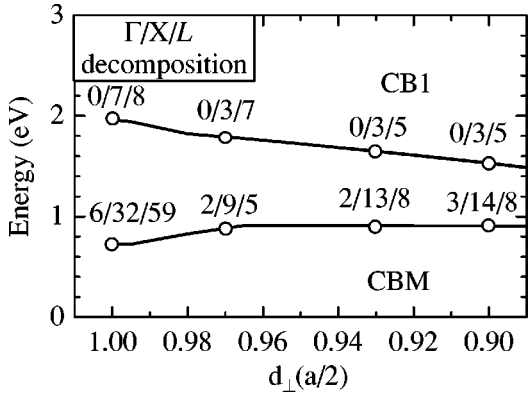

FIG. 9. Energetical position of the CBM and CB1 of $GaN_{1,s}/GaAs_{m,us}$ (Fig. 6, right panel) in dependence on the vertical spacing parameter $d_\perp$ (without so-coupling correction) where $d_\perp$ varies from $a/2$ to 0.9 $a/2$. The corresponding $\Gamma/X/L$ spectral decomposition is given for $d_\perp = 1.00, 0.97, 0.93$, and 0.90 $a/2$. Here, the latter two decomposition values measure the X and L couplings due to chemical effects (N potential), Brillouin-zone folding, and size effects.

There is a striking difference between the CBM and the CB1. While the CBM is almost independent of the $d_\perp$, CB1 is shifted into the fundamental band gap with decreasing spacing parameter $d_\perp$. A similar behavior was found for the CBM of the 15 ML (001) supercells containing a single strained GaAs monolayer (Fig. 6, left panel). In addition, the influence of chemical effects has been modeled by means of $GaN_{1,s}/GaAs_{m,us}$ structures with $d_\perp = 0.9\ a/2$ and m varying from 1 to 14. As can be seen in the right panel of Fig. 7, for $m > 5$, the energetical position of CBM and CB1 is approximately constant. This suggests that already for $m > 5$, i.e., for a 1.5-nm-thick GaAs spacing layer, the substitution layers are electronically decoupled. This result is in good correspondence with the calculated 1.5 nm spread of the weakly localized tail of the N impurity $a_1(N)$ wave functions in III–V alloys containing N impurities.[46] Recalling from Ref. 6 that periodically arranged In atomic substitution layers are electronically decoupled only for 5-nm-thick GaAs spacing layers, we conclude that a nitrogen substitution layer introduces a very short-ranged potential in the GaAs host material. For $m < 5$, the energetical position of the CBM (CB1) decreases (increases) with decreasing m. According to the small shift of the energetical position of the CBM and CB1 in dependence on m (Fig. 7, left panel), the $GaAs_{1,s}/GaAs_{m,us}$ structure shows nearly no electronic coupling. Therefore, the BGR is a genuinely chemical and not a supercell effect. Figures 8 and 9 show the spectral projection of the CBM and CB1 of the $GaN_{1,s}/GaAs_{14,us}$ and $GaAs_{1,s}/GaAs_{13,us}$ structures, respectively, in dependence on $d_\perp$. For 15 unstrained GaAs MLs ($d_\perp = 1.00\ a/2$ in Fig. 8), the sum of the spectral $\Gamma/X/L$ projection of the CBM amounts to 100%. This coincides with the spectral projection of the CBM of the GaAs host material. For CB1, the X projection (19 %) is the only contribution to the spectral $\Gamma/X/L$ projection. Therefore, we conclude that CB1 is a state folded from X to the Γ point. As a general fact, a spectral projection being smaller than 100% indicates a localization of the corresponding state in the real space. Note that for CB1, localization occurs already for $d_\perp = 1.00\ a/2$. With the increasing strain, the two lowest conduction-bands of the $GaAs_{1,s}/GaAs_{13,us}$ structure cross, the Γ and L projections approach zero, and the X projection further decreases. This corresponds to an increasing localization of the CBM and CB1 and is consistent with the results obtained for the $GaAs_{1,s}/GaAs_{m,us}$ structure with $d_\perp = 0.9\ a/2$ (Fig. 4). By substituting one unstrained GaAs ML ($d_\perp = a/2$ in Fig. 8) by one unstrained GaN ML ($d_\perp = a/2$ in Fig. 9), we observe a redistribution of the spectral weight and attribute this to the electronic coupling between CBM and CB1. For example, for $d_\perp = a/2$ the X and L projections amount to 32% and 59%, respectively. Most remarkably, the nitrogen potential leads to a strong shift of the CBM into the GaAs band gap. Here, pressure induces a decreased admixture of $\Gamma/X/L$ states. For the studied nitrogen content of 7%, the L weight is twice as large as the X weight (Fig. 9). This is in correspondence with the results of Szwacki and Boguslawski.[18] They point out that in GaAsN alloys, the impurity-induced coupling of states from various points of the Brillouin zone to the lowest conduction-band alloy state E_0 is monitored by a nonlinear pressure dependence of E_0, stemming from a L_{1c} coupling at low pressures and a dominant X_{1c} coupling at pressures higher than 6 GPa. The CBM of totally ordered GaAsN alloys, i.e., for example, of $GaN_{1,s}/GaAs_{14,us}$ (Fig. 9) reveals that for a pressure of ca. 1 GPa, i.e., for $d_\perp > 0.98\ a/2$, the X coupling dominates the L coupling. The total spectral weight for unstrained GaN substitution layers amounts to 97% and decreases considerably with increasing pressure. This is in correspondence with the weak CBM localization in supercells containing one unstrained GaN substitution layer (Fig. 5) and the strongly enhanced localization in supercells containing strained GaN substitution layers (Fig. 3). We remark that the localization of E_0 in GaAsN alloys also increases appreciably with increasing pressure.[16,17]

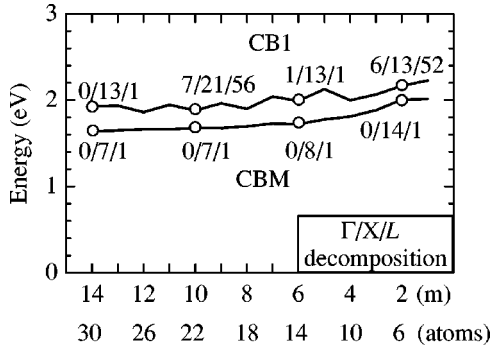

FIG. 10. Energetical position of the CBM and CB1 of $GaAs_{1,s}/GaAs_{m,us}$ (Fig. 7, left panel) as a function of the supercell size m. The corresponding $\Gamma/X/L$ spectral decomposition is given for $m=2,6,10$, and 14. Here the latter two decomposition values measure the X and L coupling due to Brillouin-zone folding and size effects (not to chemical effects).

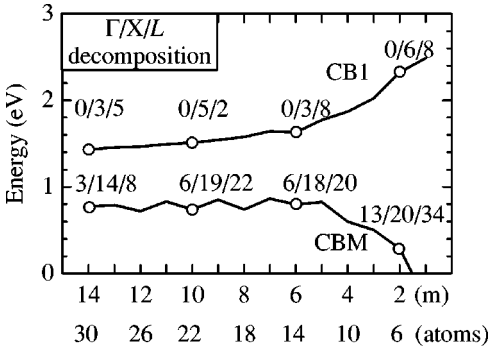

FIG. 11. Energetical position of the CBM and CB1 of $GaN_{1,s}/GaAs_{m,us}$ (Fig. 7, right panel) as a function of the supercell size m. The corresponding $\Gamma/X/L$ spectral decomposition is given for $m=2,6,10$, and 14. The latter two decomposition values measure the X and L couplings due to chemical effects (N potential), Brillouin-zone folding and size effects.

Finally, let us discuss the origin of the second lowest conduction band CB1 of a GaAs/GaN superlattice in connection with the controversy regarding the origin of the second lowest conduction-band state E_+ in GaAsN alloys. According to Hjalmarson *et al.*,[19] an isolated N impurity in GaAs induces a resonance $a_1(N)$, which is situated above the bottom of the conduction band and is mainly localized on the neighbors. With increasing concentration of N, the energy of $a_1(N)$ rises and another state develops into the second lowest conduction band and further on into the nonlocalized $a_1(L_{1c})$ from the secondary minimum of L. As in GaAsN alloys, the CB1 of GaN/GaAs behaves like a resonance that in this system is induced by isolated two-dimensional N substitution layers. This resonance is situated 0.08 eV below the GaAs host material conduction-band minimum (Fig. 2) and increases in energy with decreasing substitution layer distance, i.e., with increasing N content. Furthermore, Fig. 5 clearly shows that this resonance is localized around the substitution layer.

It should be noted that the reduction of symmetry in a GaAsN alloy is too low to have an impact on the band structure in dependence on the nitrogen content. However, for two-dimensional nitrogen substitution layers in GaN/GaAs superlattices, one has to take into account that symmetry effects can superimpose the nitrogen induced effects. The spectral projection of the CBM and CB1 in dependence on m clearly answers the question whether CBM-L and CBM-X couplings (symmetry effect) or the chemical effects cause the huge band-gap reduction in GaN/GaAs superlattices. In Figs. 10 and 11, the spectral projection of the $GaAs_{1,s}/GaAs_{m,us}$ structure and of the $GaN_{1,s}/GaAs_{m,us}$ structure, respectively, is represented for $d_\perp=0.9\ a/2$ in dependence on m. The X-weight fluctuations of the CB1 in Fig. 10 amount to one-quarter of the corresponding L-weight fluctuations. The spectral X- and L-weight fluctuations of the CBM in Fig. 11 are equal and can be correlated with the corresponding fluctuating energetical position (Fig. 10). These fluctuations can be explained by a symmetry dependent folding of Brillouin zone states to the Γ point.[49]

As a side-effect, these fluctuations can also be considered as an indicator for the former CBM state of the GaAs host material. Wang and Zunger[49] discuss symmetry effects, i.e., the fluctuations of the Γ_{1c}-X_{3c} and Γ_{1c}-X_{1c} couplings and the energetical position of the Γ_{1c} state in cation-substituted $AlAs_n/GaAs_n$ superlattices in dependence on the superlattice period n. (Note the exchanged notation of X_{1c} and X_{3c} in anion-substituted superlattices, for example, $GaN_1/GaAs_m$, with respect to cation-substituted superlattices, for example, $AlAs_n/GaAs_n$). Because we do not distinguish between the X_{1c} and X_{3c} weights, we can directly compare our results with the results obtained on cation-substituted superlattices.[49] Wang and Zunger state that the Γ_{1c}-X_{3c} and $\Gamma_{1c}-X_{1c}$ couplings are maximum for $AlAs_n/GaAs_m$-superlattice periods $n=2,4,6$ and $n=1,3,5,7$, respectively. This should be reflected in $GaN_{1,s}/GaAs_{14,us}$ energy peaks for $m=3,7,11$ and $m=1,5,9,13$, respectively. For $m>5$, we observe the expected fluctuations in dependence on m. For $m<5$, we observe additional coupling effects due to the higher symmetry of small superlattices.[50]

The fact that the two lowest conduction-bands of the GaAs/GaAs system (Fig. 8) cross at $d_\perp=0.97\ a/2$ and that the CB1 state of the GaN/GaAs system (Fig. 11) and the CBM state of the GaAs/GaAs system (Fig. 10) have nearly the same energetical position at the same $d_\perp$ value confirms our assumption about the similar character of both states, already drawn from the charge-density figures (see Sec. III A). Due to the nitrogen potential, the mean spectral L weight of the CB1 in $GaN_{1,s}/GaAs_{m,us}$ is larger than that of the CBM in $GaAs_{1,s}/GaAs_{m,us}$. However, the energetical position of the CBM in Fig. 10 and of the CB1 in Fig. 11 only depends on the superlattice size and not on the nitrogen content. Since both the spectral $\Gamma/X/L$ projection of the CBM in $GaN_{1,s}/GaAs_{m,us}$ (Fig. 11) and of the CB1 in $GaAs_{1,s}/GaAs_{m,us}$ (Fig. 10) show roughly a similar dependence on the supercell size, we can exclude that the anomalously huge band-gap reduction is caused by a symmetry dependent CBM-L or CBM-X coupling. Therefore, it is the

modification of the crystal field potential due to the nitrogen substitution layer (chemical effect) that causes the huge band-gap reduction.

IV. CONCLUSIONS

The EPP calculations have been performed to investigate the effect of a single atomic nitrogen substitution layer on the electronic properties of the GaAs host material. Both the chemical and size effects associated with the embedded nitrogen layer cause a splitting of the sixfold degenerate zincblende Γ_{15}^{v} valence-band state and a huge reduction of the band gap of the GaAs host material. This band-gap reduction, the existence of *two* localized conduction-band states CBM and CB1, and the wave-function mixing in the lower conduction-band region show that the GaN/GaAs system possesses ''anomalous'' band-structure properties. We have correlated the CBM and CB1 of the GaN/GaAs system with the lowest conduction-band alloy state E_0 and the N impurity state $a_1(N)$ of GaAsN alloys, respectively. The physical origin of the band-structure anomalies of GaN/GaAs are, first, the huge tensile strain introduced by the GaN substitution layer, which causes the localization of the lowest conduction-bands around the substitution layer, and, second, the coupling between the CBM and the nitrogen potential, which causes the pushing of the CBM deep into the band gap of the GaAs host material.

Further, theoretical investigations should answer the question whether it is generally true that if an isovalent alloy exhibits band-structure anomalies, then so does any perfectly ordered superlattice with the same constituents, independent of its orientation.

ACKNOWLEDGMENTS

We acknowledge fruitful discussions with M. Schubert, R. Pickenhain, and M. Grundmann. One of us (H.S.) acknowledges financial support from the Saxon Ministry of Science and Culture (SMWK).

[1] R. Cingolani, O. Brandt, L. Tapfer, G. Scamarcio, G.C. La Rocca, and K. Ploog, Phys. Rev. B **42**, 3209 (1990).
[2] T. Makimoto and N. Kobayashi, Jpn. J. Appl. Phys., Part 1 **35**, 1299 (1996).
[3] R. Schwabe, F. Pietag, M. Faulkner, S. Lassen, V. Gottschalch, R. Franzheld, A. Bitz, and J.L. Staehli, J. Appl. Phys. **77**, 6295 (1995).
[4] J.A. Prieto, G. Armelles, M.-E. Pistol, P. Castrillo, J.P. Silveira, and F. Briones, Appl. Phys. Lett. **70**, 3449 (1997).
[5] M. Schubert, H. Schmidt, J. Šik, T. Hofmann, V. Gottschalch, W. Grill, G. Böhm, and G. Wagner, Mater. Sci. Eng., B **88**, 125 (2002).
[6] H. Schmidt, R. Pickenhain, and G. Böhm, Phys. Rev. B **65**, 045323 (2002).
[7] F. Kasahara, K. Kanazawa, N. Okamoto, H. Ikoma, Jpn. J. Appl. Phys., Part 1 **38**, 6597 (1999).
[8] S. Ruvimov, Z. Liliental-Weber, J. Washburn, T.J. Drummond, M. Hafich, and S.R. Lee, Appl. Phys. Lett. **71**, 2931 (1997).
[9] J. Jasinski, Z. Liliental-Weber, S. Estrada, and E. Hu, Appl. Phys. Lett. **81**, 3152 (2002).
[10] Y. Kribes, I. Harrison, B. Tuck, T.S. Cheng, and C.T. Foxon, J. Cryst. Growth **189/190**, 773 (1998).
[11] T. Makimoto and N. Kobayashi, Jpn. J. Appl. Phys., Part 1 **35**, 1299 (1996).
[12] T. Makimoto, H. Saito, and N. Kobayashi, Jpn. J. Appl. Phys., Part 1 **36**, 1694 (1997).
[13] Y. Zhang, A. Mascarenhas, H.P. Xin, and C.W. Tu, Phys. Rev. B **61**, 7479 (2000).
[14] P.N. Hai, W.M. Chen, I.A. Buyanova, H.P. Xin, and C.W. Tu, Appl. Phys. Lett. **77**, 1843 (2000).
[15] C. Skierbiszewski, P. Perlin, P. Wisniewski, T. Suski, W. Walukiewicz, W. Shan, J.W. Ager, E.E. Haller, J.F. Geisz, D.J. Friedman, J.M. Olson, and S.R. Kurtz, Phys. Status Solidi B **216**, 135 (1999).
[16] A. Zunger, Phys. Status Solidi B **216**, 117 (1999).
[17] T. Mattila, S.-H. Wei, and A. Zunger, Phys. Rev. B **60**, R11 245 (1999).
[18] N.G. Szwacki and P. Boguslawski, Phys. Rev. B **64**, 161201(R) (2001).
[19] H.P. Hjalmarson, J. Vac. Sci. Technol. **21**, 524 (1982).
[20] X. Huang, T.S. Cheng, S.E. Hooper, T.J. Foster, L.C. Jenkins, J. Wang, C.T. Foxon, J.W. Orton, L. Eaves, and P.C. Martin, J. Vac. Sci. Technol. B **13**, 1582 (1995).
[21] M. Sato, Jpn. J. Appl. Phys., Part 1 **34**, 1080 (1995).
[22] K. Kim, P.R.C. Kent, A. Zunger, and C.B. Geller, Phys. Rev. B **66**, 045208 (2002).
[23] R. Magri and A. Zunger, Phys. Rev. B **65**, 165302 (2002).
[24] N.W. Ashcroft, Phys. Rev. B **23**, 48 (1966).
[25] Z.H. Levine and S.G. Louie, Phys. Rev. B **25**, 6310 (1982).
[26] S.-H. Wei and A. Zunger, Phys. Rev. B **49**, 14 337 (1994).
[27] M.S. Hybertsen and S.G. Louie, Phys. Rev. B **34**, 5390 (1986).
[28] K. Shimada, T. Sota, and K. Sizuki, J. Appl. Phys. **84**, 4951 (1998).
[29] S.-H. Wei and A. Zunger, Appl. Phys. Lett. **69**, 2719 (1996).
[30] N.E. Christensen and I. Gorczyca, Phys. Rev. B **50**, 4397 (1994).
[31] *Semiconductors Physics of Group IV Elements and III-V Compounds*, edited by K.H. Hellwege and O. Madelung, Landolt-Börnstein, New Series, Group III Vol. 17 Pt. a (Springer, Berlin, 1982).
[32] H. Okomura, S. Yoshida, and T. Okahisa, Appl. Phys. Lett. **64**, 2997 (1994).
[33] W.J. Fan, M.F. Li, T.C. Chong, and J.B. Xia, J. Appl. Phys. **79**, 188 (1996).
[34] G. Böhm and K. Unger, Phys. Status Solidi B **216**, 961 (1999).
[35] F. Aymerich and G. Mula, J. Phys. C **9**, 3217 (1976).
[36] B.L. Sharma and R.K. Purohit, *Semiconductor Heterojunctions* (Pergamon, Oxford, 1974).
[37] C.J. Wu and A. Kahn, J. Appl. Phys. **86**, 3209 (1999).
[38] S.-H. Wei and A. Zunger, Appl. Phys. Lett. **72**, 2011 (1998).

[39] J. Hornstra and W.J. Bartels, J. Cryst. Growth **44**, 513 (1978).
[40] K. Kim, W.R.L. Lambrecht, and B. Segall, Phys. Rev. B **53**, 16 310 (1996).
[41] O. Zsebök, J.V. Thordson, and T.G. Andersson, Jpn. J. Appl. Phys., Part 1 **40**, 472 (2001).
[42] Z.Z. Bandić, R.J. Hauenstein, M.L. O'Steen, and T.C. Mc Gill, Appl. Phys. Lett. **68**, 1510 (1996).
[43] D.P. Xu, Y.T. Wang, H. Yang, S.F. Li, D.G. Zhao, Y. Fu, S.M. Zhang, R.H. Wu, Q.J. Jia, L. Zheng, and X.M. Jiang, J. Appl. Phys. **88**, 3762 (2000).
[44] L.-W. Wang and A. Zunger, J. Chem. Phys. **100**, 2394 (1994).
[45] A. Baldereschi, S. Baroni, and R. Resta, Phys. Rev. Lett. **61**, 734 (1988).
[46] L.-W. Wang, Phys. Rev. B **78**, 1565 (2001).
[47] P.R.C. Kent and A. Zunger, Phys. Rev. Lett. **86**, 2613 (2001).
[48] P.R.C. Kent, G.L.W. Hart, and A. Zunger, Appl. Phys. Lett. **81**, 4377 (2002).
[49] L.-W. Wang and A. Zunger, Phys. Rev. B **56**, 12 395 (1997).
[50] Y.E. Kitaev, A.G. Panfilov, P. Tronc, and R.A. Evarestov, J. Phys.: Condens. Matter **9**, 257 (1997).